Structural Investigations of the Catalytic Mechanisms of Water Oxidation by the $[(bpy)_2Ru(OH_2)]_2O^{4+}$ Ion

Yabin Lei[‡] and James K. Hurst[*,†]

Department of Chemistry, Biochemistry, and Molecular Biology, Oregon Graduate Institute of Science and Technology, P.O. Box 91000, Portland, Oregon 97291-1000

Received September 2, 1993[⊗]

Electron paramagnetic resonance and Raman spectroscopies have been used to identify component species in acidic solutions containing the water oxidation catalyst (μ-oxo)bis[*cis*-aquabis(2,2′-bipyridine)ruthenium(III)] ([3,3]) and Ce^{4+} ions. One-electron oxidation with Ce^{4+} gave rise to an anisotropic pH-dependent EPR signal at g = 1.77−1.90, assigned to the $S = {}^1/_2$ ground state of a spin-delocalized Ru−O−Ru orbital. Appearance of the EPR signal correlated with formation of a resonance-enhanced symmetric band at 405−410 cm^{-1} in the Raman spectrum, attributable to the Ru−O−Ru symmetric (ν_s) stretching mode. Upon further addition of Ce^{4+} in 0.1 M acid, a second anisotropic EPR signal was detected at g = 1.87, which correlated with a ν_s(Ru−O−Ru) band appearing at 398 cm^{-1}. By analogy with the one-electron oxidation product ([3,4]), this species was assigned as the $S = {}^1/_2$ three-electron oxidized ion ([4,5]). In 1 M acid, however, the EPR spectrum of highly oxidized samples also exhibited an unusual isotropic signal centered at g = 1.95, whose relative intensity correlated with resonance Raman bands at ~357 cm^{-1} (ν_s(Ru−O−Ru)) and 817 cm^{-1} (ν(Ru=O)). By analogy with very similar signals reported for reduced $Ru(bpy)_3^+$ ions and related species which contain bipyridine radical anions as ligands, the g = 1.95 signal is tentatively assigned to a coordinated bipyridine radical *π-cation* in a complex whose metal oxidation state is [5,5].

Introduction

Oxo-bridged ruthenium dimers of the type $(cis\text{-}L_2RuOH_2)_2O$, where L is 2,2′-bipyridine or a ring-substituted analog, exhibit remarkable catalytic capabilities toward the oxidation of water.[1−11] These reactions are fundamentally interesting from the point of view of understanding mechanisms by which redox metal clusters can obviate reactant noncomplementarity[12] and in relation to biological water oxidation, particularly since manganese clusters that effectively mimic the structural features of the oxygen-evolving complex of photosystem II are catalytically inactive.[13] There is also critical need for development of catalysts that can close oxidative half-cycles in solar photoconversion/photostorage systems and related technologies based upon photoredox chemistry.[14,15]

Although the ruthenium μ-oxo dimers have been fairly extensively studied as catalysts, there is as yet no clear understanding of their reaction mechanisms. For example, neither the oxidation state(s) of the catalytically active species nor the immediate oxidized product (H_2O_2, HO_2, or O_2) has been identified. In addition to the $(Ru(bpy)_2OH_2)_2O^{4+}$ [3,3] ion,[16] the [3,4], [4,5], and [5,5] ions have all been characterized by electrochemical measurements and for the 4,4′-carboxybipyridine analog, the [4,4] ion has been generated transiently by pulse radiolysis.[8] The [4,4], [4,5], and [5,5] ions have all in various reports been proposed as catalytically active forms.[1,4,6−8] The higher oxidation states are stabilized by $p_\pi-d_\pi$ backbonding from deprotonated *cis*-aqua ligands;[1,10,12] in the [5,5] ion, at least, these ligands appear to be completely converted to terminal ruthenyl oxo groups.[10] Early mechanistic speculations generally invoked intramolecular reductive elimination of the *cis*-oxo or hydroxo ligands from the highly oxidized dimers, forming O_2 or H_2O_2 directly.[1,4,7,8] However, ^{18}O-isotopic labeling studies showed that these pathways are unimportant.[9,10] In $(Ru(bpy)_2OH_2)_2O$-catalyzed oxidations of water by Ce^{4+} and Co^{3+} ions, approximately half of the O_2 produced contained one oxygen atom obtained from the *cis*-aqua ligand and the other obtained from solvent; for the remainder of the O_2 formed, both atoms of oxygen came from the solvent. These results clearly

* To whom correspondence should be addressed.
† Current address: Department of Chemistry, Washington State University, Pullman, WA 99164.
‡ Current address: Department of Chemistry, California Institute of Technology, Pasadena, CA 91125.
⊗ Abstract published in *Advance ACS Abstracts,* August 1, 1994.

(1) Gilbert, J. A.; Eggleston, D. S.; Murphy, W. H., Jr.; Geselowitz, D. A.; Gersten, S. W.; Hodgson, D. J.; Meyer, T. J. *J. Am. Chem. Soc.* **1985**, *107*, 3855.
(2) Honda, K. J.; Frank, A. J. *J. Chem. Soc., Chem. Commun.* **1984**, 1635.
(3) Collin, J. P.; Sauvage, J. P. *Inorg. Chem.* **1986**, *25*, 135.
(4) Rotzinger, F. P.; Munavalli, S. P.; Comte, P.; Hurst, J. K.; Grätzel, M.; Pern, F-J.; Frank, A. J. *J. Am. Chem. Soc.* **1987**, *109*, 6619.
(5) Doppelt, P.; Meyer, T. J. *Inorg. Chem.* **1987**, *26*, 2027.
(6) Raven, S. J.; Meyer, T. J. *Inorg. Chem.* **1988**, *27*, 4478.
(7) Nazeeruddin, M. K.; Rotzinger, F. P.; Comte, P.; Grätzel, M. *J. Chem. Soc., Chem. Commun.* **1988**, 872.
(8) Comte, P.; Nazeeruddin, M. K.; Rotzinger, F. P.; Frank, A. J.; Grätzel, M. *J. Mol. Catal.* **1989**, *52*, 63.
(9) Geselowitz, D.; Meyer, T. J. *Inorg. Chem.* **1990**, *29*, 3894.
(10) Hurst, J. K.; Zhou, J.; Lei, Y. *Inorg. Chem.* **1992**, *31*, 1010.
(11) Petach, H. H.; Elliott, C. M. *J. Electrochem. Soc.* **1992**, *139*, 2217.
(12) See, e.g., Meyer, T. J.; *J. Electrochem. Soc.* **1984**, *131*, 221C.
(13) See, e.g., Wieghardt, K. *Angew. Chem., Int. Ed. Engl.* **1989**, *28*, 1153 and references cited therein.
(14) Grätzel, M., Ed., *Energy Resources Through Photochemistry and Catalysis*; Academic Press: New York, 1983.
(15) Connolly, J. S., Ed.; *Photochemical Conversion and Storage of Solar Energy*; Academic Press: New York, 1981.
(16) This notation is intended to imply the net oxidation level of the μ-oxo ions only. Meyer and co-workers have presented convincing arguments that the physical properties of these ions are best described by models in which the electrons are extensively delocalized over a Ru−O−Ru three-center bond.[17] Thus, e.g., the notation [3,4] is not meant to imply charge-localized mixed-valence complex comprising discrete ruthenium d^4 and d^5 ions, but rather an oxidation level for which the Ru−O−Ru unit contains 13 π-electrons (with four from O^{2-}). Similarly, in the [3,3] ion there are 14 π-electrons in the Ru−O−Ru unit, etc.
(17) Weaver, T. R.; Meyer, T. J.; Adeyemi, S. A.; Brown, G. M.; Eckberg, R. P.; Hatfield, W. E.; Johnson, E. C.; Murray, R. W.; Untereker, D. *J. Am. Chem. Soc.* **1975**, *97*, 3039.

0020-1669/94/1333-4460$04.50/0

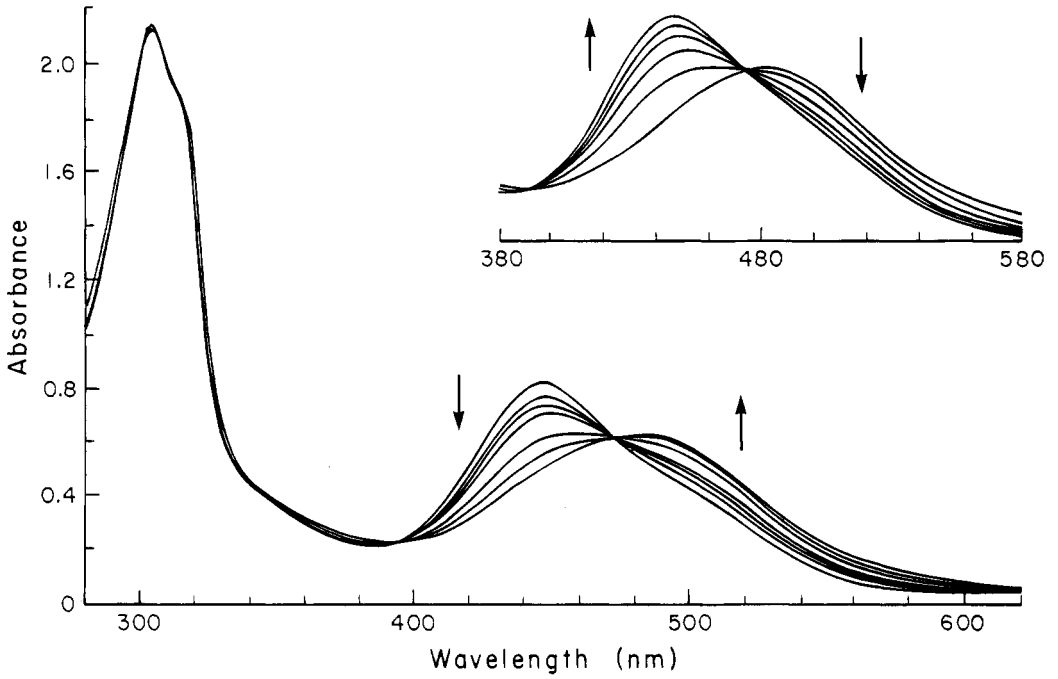

Figure 1. Optical spectral changes upon oxidation of the $(Ru(bpy)_2OH_2)_2O^{4+}$ [3,4] ion with Ce^{4+}. Incremental additions of 2.3, 4.5, 6.0, 8.0, 10, 12, and 15 oxidizing equiv of Ce^{4+} were made to 195 μM of the [3,3] μ-oxo dimer in 1 M CF_3SO_3H. The arrows indicate the progression of change in the spectra, which were corrected for dilution. The inset shows changes in the visible spectral region over a 2-h period following addition of a 15-fold excess of Ce^{4+} ion.

indicate that an important aspect of catalysis in these complexes is solvent activation. This conclusion is supported by additional studies reporting catalysis of water oxidation by asymmetric ruthenium μ-oxo ions containing only one *cis*-aqua ligand[5] and by sterically constrained μ-oxo ions for which it is believed that close approach of the two *cis*-oxo ligands is energetically prohibitive.[11]

In this paper, we use resonance Raman (RR) and EPR spectroscopy to characterize the species formed upon oxidation of the $(Ru(bpy)_2OH_2)_2O^{4+}$ μ-oxo ion. These studies clearly demonstrate that the number of species present under highly oxidizing conditions is greater than has heretofore been recognized and that RR and EPR methods constitute powerful techniques for quantitating ruthenium component distributions in these complex mixtures.

Experimental Section

Materials. The perchlorate salt of the coordination complex (μ-oxo)bis[*cis*-aquabis(2,2′-bipyridine)ruthenium(III)] (or $(Ru(bpy)_2OH_2)_2O^{4+}$) was synthesized from $(bpy)_2RuCl_2$, as described by Meyer and coworkers, and recrystallized three times from aqueous perchloric acid.[1] (*Caution*! the perchlorate salts of these complexes are potentially explosive!) Reagent solutions were prepared fresh daily as required and standardized by spectrophotometric analysis. Optical band positions and extinction coefficients agreed with previously reported values.[1] Trifluoromethane sulfuric acid (3M Corp.) was purified by vacuum distillation and stored as ~2 M aqueous solutions. Ceric ion solutions were prepared fresh daily as required by dissolving weighed amounts of $(NH_4)_2Ce(NO_3)_6$ in aqueous CF_3SO_3H. Solutions containing higher oxidation states of the $(Ru(bpy)_2OH_2)_2O$ ions were prepared by constant potential electrolysis (CPE), and the reaction course was followed by periodically recording the optical absorption spectra.[1,10] Other reagents were best-available grade and used as received. All solutions were prepared from H_2O that had been purified by reverse osmosis/ion-exchange chromatography; for kinetic studies, this water was additionally purified by distillation from quartz.

Methods. Raman spectra were recorded on a computer-controlled Jarrell-Ash instrument[18] with excitation from a Spectra Physics Model 164 argon ion laser. Solutions of $(Ru(bpy)_2OH_2)_2O^{4+}$ were oxidized with Ce^{4+} at 4 °C in a cold room. Immediately following addition of the oxidant, samples for Raman analyses were transferred to capillary tubes, which were then sealed and immersed in liquid nitrogen. Spectra were determined by collecting and analyzing backscattered photons from the samples, which were maintained at 90 K by mounting the tubes in a slotted copper cold finger in contact with a liquid N_2 bath contained within a Dewar flask.

Low-temperature electron paramagnetic resonance spectra were obtained with a Varian Model E-109 X-band instrument equipped with an Air Products Model LTR liquid-helium cryostat. The output signal was digitized using a Keithley Model 195A digital multimeter and transferred via an IO Tech MAC4A bus controller to an Apple Macintosh II computer for data analysis and storage. No magnetic field standards were used, although the accuracy of the instrument field dial was confirmed to less than 0.1% error over the range 1000−5000 G by calibration with a Varian NMR gaussmeter. Optical spectra were recorded with a Hewlett-Packard 8452A diode-array spectrophotometer interfaced to a Hewlett-Packard 89500 ChemStation data analysis/acquisition system. Electrochemical oxidations were made with a computer-controlled PAR Model 273 potentiostat/galvanostat.

Results

Resonance Raman Spectral Titrations. Optical spectroscopic changes that occurred during Ce^{4+} titration of the $(Ru(bpy)_2OH_2)_2O^{5+}$ ion (hereafter, designated as the [3,4] ion[16]) are illustrated in Figure 1. Progressive loss of intensity in the band at 446 nm was accompanied by the appearance of a new band at ~482 nm; isosbestic points were observed at 470 and ~393 nm. On the basis of a molar extinction coefficient, $\epsilon_{446} = 2.4 \times 10^4\ M^{-1}\ cm^{-1}$, for the [3,4] ion, the apparent extinction coefficient for the new band was calculated from three separate measurements to be $1.5 \times 10^4\ M^{-1}\ cm^{-1}$.

Raman spectral changes observed under 488 nm excitation at various levels of oxidation by Ce^{4+} ion in 1 M CF_3SO_3H are reproduced in Figure 2. The dominant feature of these spectra was the Ru—O—Ru symmetric stretching band (ν_s), which appeared at 405 cm^{-1} for the [3,4] ion.[10] This band decreased progressively in intensity with addition of increasing amounts

(18) Loehr, T. M., Keyes, W. E.; Pincus, P. A. *Anal. Biochem.* **1979**, *96*, 456.

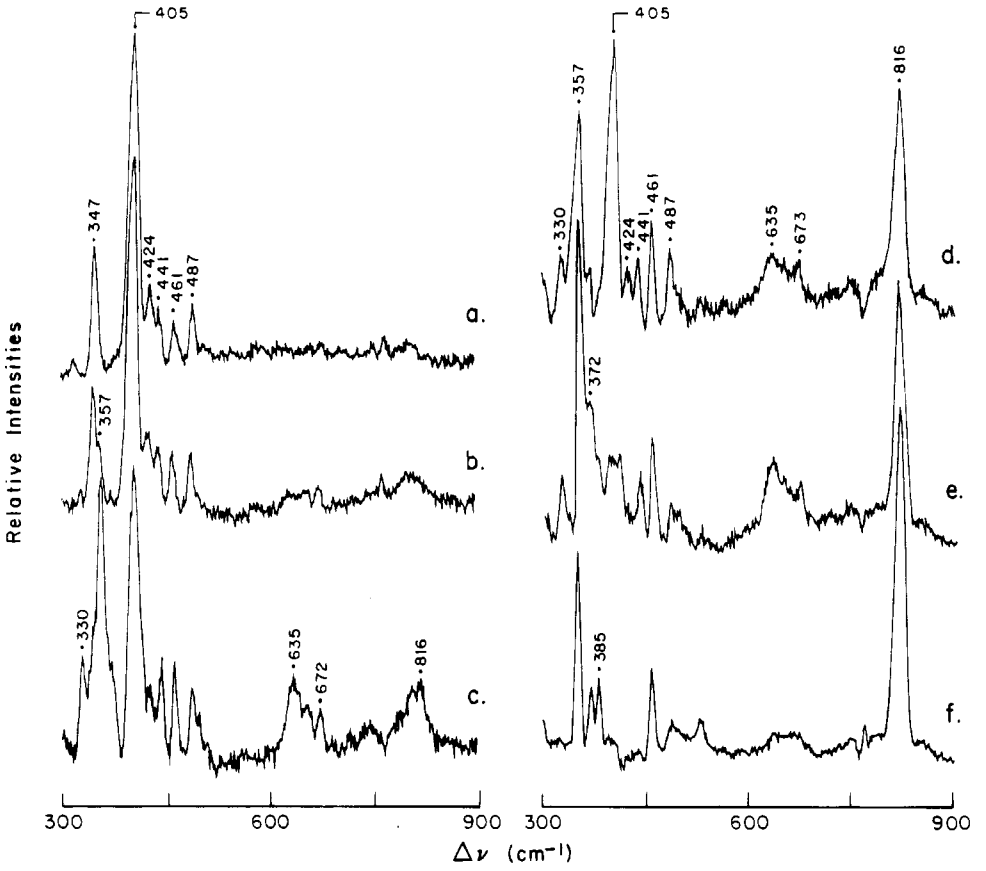

Figure 2. Resonance Raman spectra of Ce^{4+}-oxidized $(Ru(bpy)_2OH_2)_2O^{4+}$ ions. Spectra a–f correspond to additions of 2, 4, 6, 8, 10, and 11 equiv of Ce^{4+}, respectively, at 4 °C to 200 μM $(Ru(bpy)_2OH_2)_2O^{4+}$ ion in 1 M CF_3SO_3H. Spectra taken following addition of 1 equiv of Ce^{4+} were identical to spectrum a and, with 14 equiv Ce^{4+}, to spectrum f. Spectra displayed are averages of six scans taken at 10 mW-excitation at 488 nm, with a 7-cm^{-1} slit width and 1 cm^{-1}/s scan rate. The normal Raman spectrum of CF_3SO_3H, which gives medium-to-strong scattering at 319, 353, 583, 767, and 1037 cm^{-1}, has been computer-subtracted, but data smoothing routines were not applied.

of Ce^{4+} ion. Major new spectral features that emerged were a second Ru—O—Ru ν_s band at 355–357 cm^{-1} and a strong band at 816 cm^{-1} that has been assigned as a terminal ruthenyl (Ru=O) stretching mode on the basis of ^{18}O-isotopic shifts.[10] In these oxidative titrations, it was frequently noted that the 357-cm^{-1} band developed intensity sooner than the 816-cm^{-1} band. This behavior is apparent in Figure 2 from (1) comparisons of the relative intensities of the two bands at intermediary levels of oxidation (cf. Figure 2c–e) and (2) titrimetric plots of relative intensities scaled to the strong normal Raman band of CF_3SO_3H at 1037 cm^{-1}, which served as a convenient internal standard for scattering intensities (Figure 3). At the highest achievable oxidation levels, the excitation profiles for the 818- and 357-cm^{-1} bands both matched the 482-cm^{-1} absorption band (Figure 4, where the excitation wavelength-invariant I_{818}/I_{357} ratio indicates that the excitation profiles of the two bands were identical). Thus, both bands are attributable to the chromophore giving rise to the 482-cm^{-1} optical band.

Resonance Raman spectral titrations were also carried out in 0.1 M CF_3SO_3H. Under these conditions, addition of several oxidizing equivalents of Ce^{4+} caused the ν_s(Ru—O—Ru) band of the [3,4] ion at 410 cm^{-1} to decrease in intensity and new bands to appear at 398, 817, and 372 cm^{-1} (in order of decreasing intensities). The 817/372 intensity ratio was about 2.0, which is nearly identical to the 816/356 ratio measured in 1 M acid (Figure 2f). In addition, a prominent set of bands with medium intensity appeared at 653, 665, and 678 cm^{-1}; similar, although weaker, bands appeared at 635 and 673 cm^{-1} in the RR spectra at intermediary oxidation levels in 1 M CF_3SO_3H (Figure 2c–e). The RR spectra in 0.1 M CF_3SO_3H were unchanged by further additions of Ce^{4+} ion to levels as high as 12 oxidizing equiv per ruthenium.

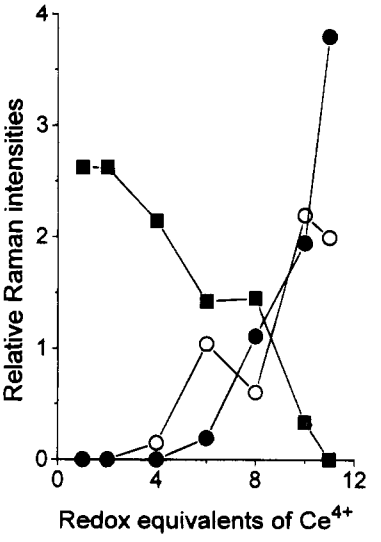

Figure 3. Dependence of scattering intensities (I) of major RR bands upon the amount of added Ce^{4+} ion. Peak amplitudes were normalized to the intensity of the CF_3SO_3H 1037-cm^{-1} band. Symbols: open circle, I_{357}/I_{1038}; closed circle, I_{818}/I_{1038}; closed square, I_{405}/I_{1038}. The intensity of the 357-cm^{-1} band required correction for contributions from overlapping bands from the [3,4] ion at 347 cm^{-1} (Figure 2a) and from CF_3SO_3H at 353 cm^{-1} and was therefore relatively innacurate at intermediary levels of oxidation.

The samples were examined for photodecomposition in the laser beam by comparing overlays of RR spectra taken as rapid

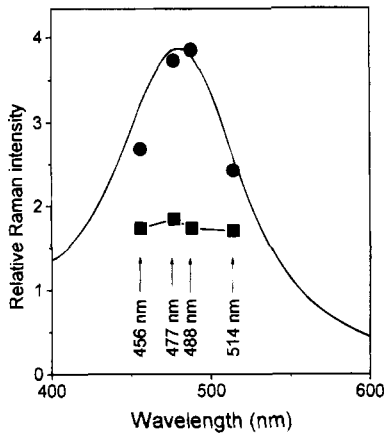

Figure 4. Excitation profiles for the highly-oxidized ruthenium μ-oxo dimer in 1 M CF_3SO_3H. Conditions: 200 μM $(Ru(bpy)_2OH_2)_2O^{4+}$; 2.2 mM Ce^{4+} ion. The normalized intensities of the 818-cm^{-1} band (circles) excited at the indicated wavelengths are overlaid by the optical absorption band (λ_{max} = 481 nm); the ratios of the 818- and 357-cm^{-1} band intensities are given by the squares.

repetitive scans over the regions 300−500 and 700−900 cm^{-1} and by comparing spectra taken at low (10 mW) and high (75 mW) incident light intensities. Band shapes and scattering intensities of the spectra of samples in 1 M CF_3SO_3H were unchanged by these variations in data collection parameters, indicating that photodegradation was negligible under these conditions. Furthermore, the RR spectrum of $(Ru(bpy)_2H_2O)_2O$ in product solutions following catalytic oxidation of H_2O with an 11-fold excess of Ce^{4+} ion was identical to spectra of the [3,4] ion. In 0.1 M CF_3SO_3H, however, slow photoreduction of the higher oxidation state was observed, as indicated by progressive loss of intensity in the 372-, 398-, and 817-cm^{-1} bands, with a corresponding increase in intensity of the 410-cm^{-1} ν_s(Ru—O—Ru) band for the [3,4] ion. The extent of this photoreduction was more pronounced when 0.9 M sodium trifluoromethanesulfonate was added to the medium.

Electron Paramagnetic Resonance Spectra. No EPR signals were detected for the [3,3] ion under any experimental conditions, including temperatures as low as 4−5 K. However, the [3,4] ion gave broad anisotropic signals at temperatures below ~20 K whose first-derivative bandshapes were similar to spectra exhibited by rhombic $S = {}^1/_2$ systems (Figure 5). The band intensities and g values of the peak maxima varied with solution acidities as follows: (1) from $[H^+]$ = 0.1−2 M, g_{max} = 1.77, while between pH 0−1, the intensity of this band increased 5-fold with decreasing solution acidity; (2) at pH 2, the peak position shifted to g = 1.80 and was constant over the range pH 2−3, although the band intensity increased another 2-fold upon decreasing the acidity; (3) at pH 4, the peak position shifted to g = 1.90 without undergoing any change in intensity; no further changes occurred upon raising the pH to 7.0. Representative EPR spectra of the [3,4] ion in each of these three acidity regions are displayed in Figure 5, where the signals have been normalized to give identical maximal intensities. The band shapes and peak positions were independent of solution composition (CF_3SO_3H, $HClO_4$), method of preparation (Ce^{4+} oxidation, constant potential electrolysis (CPE), or, at pH 6, HOCl oxidation), and instrument parameters (microwave power 0.2−180 mW, temperature 5−20 K). However, additional bands of variable intensity and position were occasionally observed in samples prepared by electrolysis for prolonged periods and in alkaline media (pH > 9). Similarly, the weak bands appearing between 2.3−3.1 kG in Figure 5 exhibited preparation-to-preparation variations, and so cannot be assigned to the [3,4] ion. No signals were found at lower fields in any

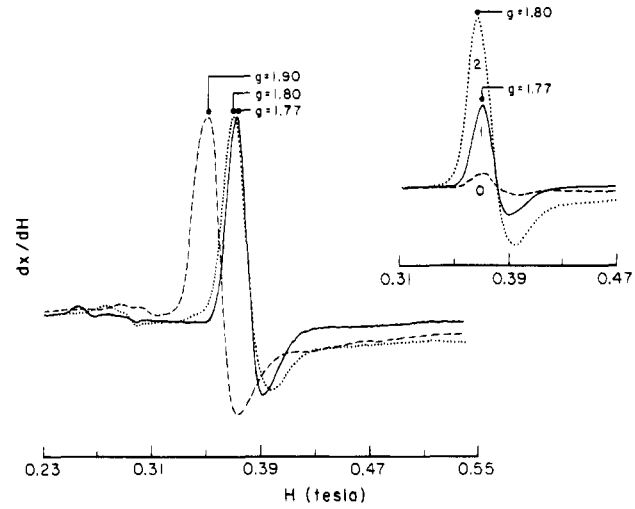

Figure 5. X-Band EPR spectra of the [3,4] ion: solid line, pH 1; dotted line, pH 2.8; dashed line; pH 4. Conditions: 900 μM [3,3] ion plus 1.2 equiv of Ce^{4+} ion at pH 0, followed by pH adjustment; T = 5 K; 9.297-GHz microwave frequency, 2-mW microwave power; 2.0-mT modulation amplitude; 1.0 T/min scan rate. Spectra were normalized to give equal peak intensities. Inset: EPR spectra in the strongly acidic region recorded at identical instrument gain settings. The numbers within the peaks indicate the solution pH values.

of the samples examined. Power saturation studies were made on the g = 1.90 band using 0.1 M phosphate solutions, pH 6, containing 1 mM [3,4] ion; from plots of log $(S/P^{1/2})$ versus log P, where S is the signal amplitude and P the applied microwave power, half-saturation values ($P_{1/2}$) were determined to be ≃16 mW at 4−5 K.[19] The signal intensities decreased with increasing temperature and were not detectable above 80 K.

Oxidation of the [3,4] ion with excess Ce^{4+} in 0.1 M CF_3SO_3H caused appearance of a prominent new signal with a g_{max} = 1.87 (Figure 6a); at pH 6, addition of a severalfold excess of HOCl or CPE at 0.7 V vs $Hg/HgSO_4$ caused partial conversion to a species with an EPR signal maximum at $g \simeq 2.02$. These bands were much less evident when the [3,4] ion was oxidized in 1 M CF_3SO_3H. Instead, a relatively narrow symmetric signal appeared at g = 1.95, which increased in relative intensity upon addition of increasing amounts of oxidant. These features are illustrated in Figure 6b,c for incremental additions of Ce^{4+} ion. The relative intensities of the g = 1.95 and g = 1.87 signals were not reproducible; in general, addition of Ce^{4+} beyond an approximate 10-fold molar excess caused the intensity of the 1.87 signal to increase relative to the g = 1.95 signal (cf. Figure 6b,c). Warming the solutions to room temperature for 5−10 min caused the optical, RR, and EPR spectra to revert to those characteristic of the [3,4] ion; both g = 1.95 and g = 1.87 EPR signals disappeared and the g = 1.77 signal reappeared in the low-temperature spectrum.

The relative intensities of the 398-cm^{-1} RR band and the g = 1.87 EPR signal in 0.1 M CF_3SO_3H roughly parallelled each other at various levels of Ce^{4+} oxidation; similarly, the intensities of the 816-cm^{-1} band and g = 1.95 signal appeared correlated in 1 M CF_3SO_3H.

Discussion

Electronic Structure of the Ru—O—Ru Bond. Several researchers have described the μ-oxo bridge in M—O—M complexes in terms of electronic delocalization of metal d_π and

(19) See, e.g.: Beinert, H.; Orme-Johnson, W. H. In *Magnetic Resonance in Biological Systems*; Ehrenberg, A., Malmström, B. G., Vänngard, T., Eds.; Pergamon Press: Oxford, England, 1976; p 221.

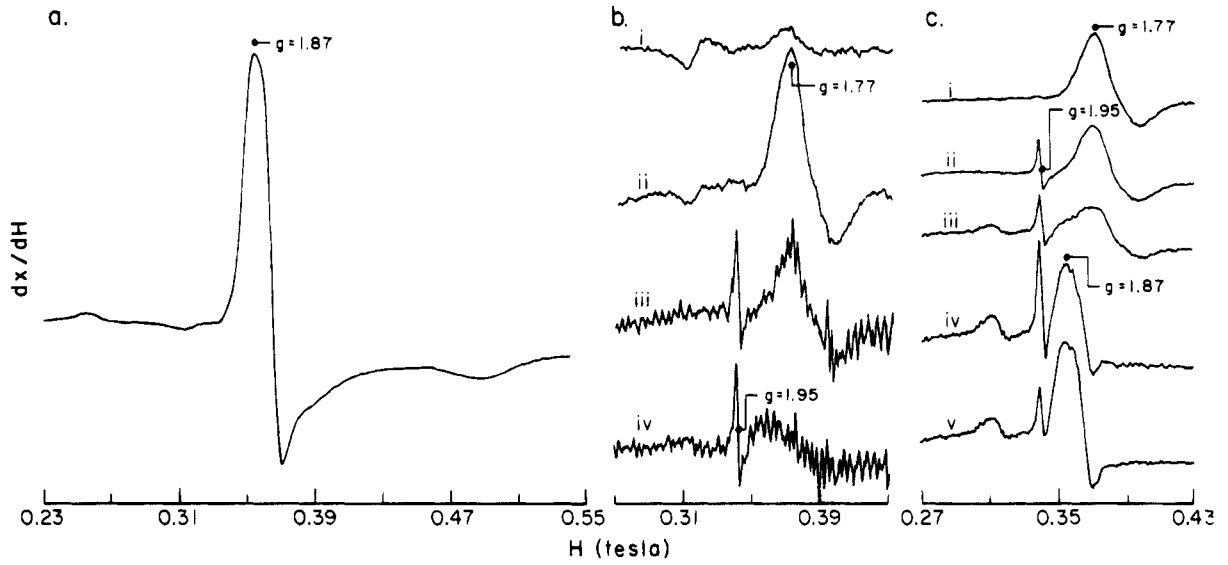

Figure 6. X-Band EPR spectra of highly oxidized ruthenium μ-oxo dimers: (a) 600 μM [3,3] plus 8 equiv of Ce^{4+} ion in 0.1 M CF_3SO_3H; (b) 900 μM [3,3] plus (i–iv) 0, 2, 6, and 10 equiv of Ce^{4+}, respectively, in 1 M CF_3SO_3H; (c) 1.5 mM [3,3] plus (i–v) 2, 4, 8, 11, and 16 equiv of Ce^{4+}, respectively, in 1 M CF_3SO_3H. Instrumental conditions are given in Figure 5. A broad band at $H = 0.2–0.3$ T attributable to Ce^{3+} ion was computer-subtracted from the spectra in panels b and c by using $CeCl_3$ in 1 M CF_3SO_3H as a reference spectrum.

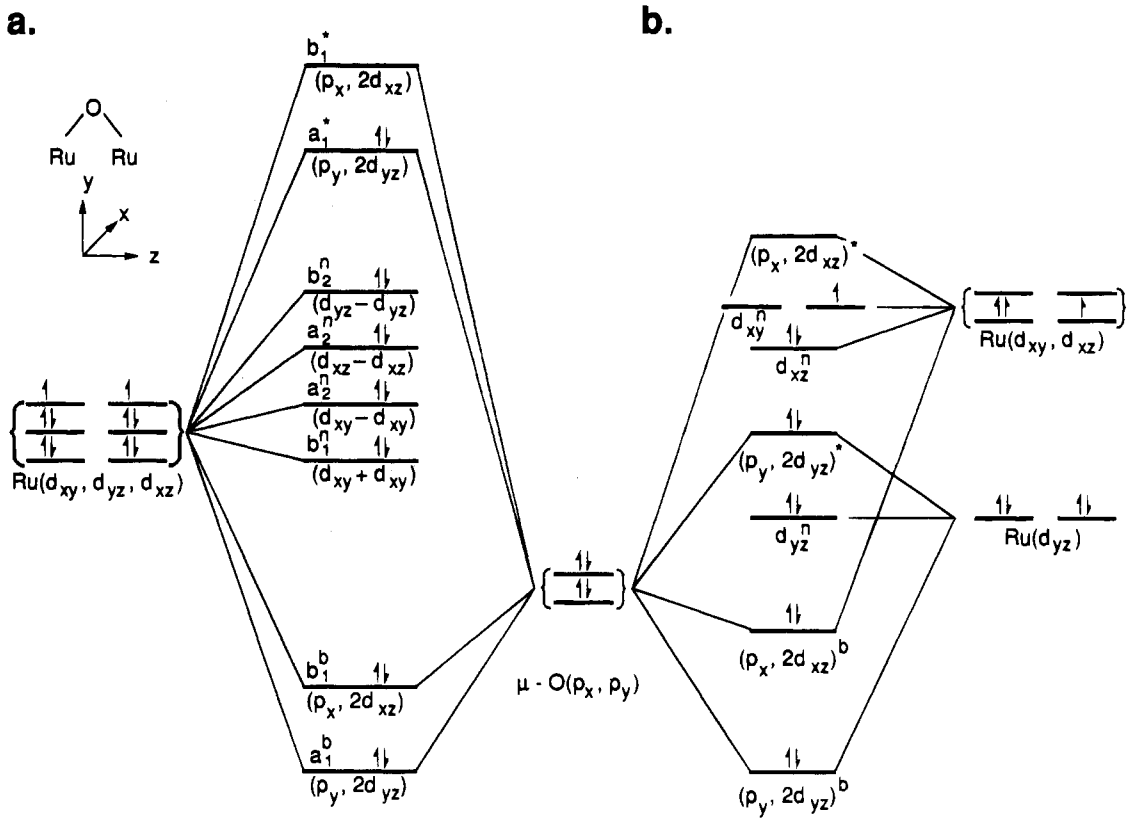

Figure 7. π-Orbital energy level diagrams for the Ru—O—Ru three-center bond: (a) the [3,3] ion in C_{2v} symmetry;[22] (b) the [4,5] ion, according to Raven and Meyer.[6]

oxo p orbitals over the three-center bond.[6,17,20–22] In D_{4h} symmetry, e.g., when the bridge is linear and the remaining ligand set about each ruthenium atom is L_5, these orbital interactions lead to formation of a doubly degenerate set of molecular orbitals.[20] In the $(Ru(bpy)_2OH_2)_2O$ ions, however, the Ru—O—Ru bridge is nonlinear, as was determined for the [3,3] ion by X-ray crystallography[1] and RR spectroscopy[10] and for the higher oxidation states by RR spectroscopy.[10] Consequently, the local symmetry about the Ru—O—Ru bond can be at most C_{2v}. As illustrated in Figure 7a, the effect of bending the bridge is to remove the degeneracies of the Ru—O—Ru π-bonding and antibonding orbitals.[22] The other energy levels will also undergo splitting if bending allows direct overlap between the ruthenium d_π-orbitals. In the various oxidation states of $(Ru(bpy)_2OH_2)_2O$ examined,[10] the bridging angle was always greater than 150°, so that electronic perturbations from metal—metal interactions are likely to be minor. However, several other structural features contribute to additional sym-

(20) Dunitz, J. D.; Orgel, L. E. *J. Chem. Soc.* **1953**, 2594.
(21) Clark, R. J. H.; Franks, M. L.; Turtle, P. C. *J. Am. Chem. Soc.* **1977**, *99*, 2473.
(22) Burchfield, D. E.; Richman, R. M. *Inorg. Chem.* **1985**, *24*, 852–857.

metry lowering in these complexes, including the *cis*-N_4O environment provided by the coordinated bipyridine and aqua ligands, twisting of the $Ru(bpy)_2OH_2$ moieties along the Ru—O—Ru bond (an (aqua)O—Ru—Ru—O(aqua) torsional angle of 66° was measured crystallographically for the [3,3] ion),[1] and electronic interactions between the ruthenium d_{xy} and d_{xz} orbitals and p-orbitals of deprotonated *cis*-aqua ligands in the higher oxidation states.[6]

As illustrated in Figure 7b, d_π—p_π interactions between terminal oxo and ruthenium atoms split the energies of the basis set of d_π orbitals, which has the effect of lifting the energies of the nonbonding d_{xy} and d_{xz} orbitals relative to the Ru—O—Ru π orbitals. Although several orderings are possible, the one shown in Figure 7b was proposed[6] on the basis that it could account for the optical absorption spectrum of the [4,5] ion. More generally, Meyer and co-workers have also noted that a delocalized electron model is more suited to describing the optical and redox properties of ruthenium bipyridine μ-oxo complexes than one involving two discrete low-spin d^5 ions that are less strongly magnetically coupled through the bridging ligand.[17]

EPR and RR Spectral Assignments. The extensive electrochemical studies of Meyer's group will be used as a reference point for our spectral assignments.[1] Their data from cyclic voltammetric and differential pulse polarographic measurements were consistent with the following oxidation sequence under most conditions:

$$[3,3] \xrightarrow{-e} [3,4] \xrightarrow{-2e} [4,5] \xrightarrow{-e} [5,5]$$

Depending on the medium acidity, electron removal in the first two steps was accompanied by loss of 0—2 H^+ ions from the *cis*-aqua ligands; in the [4,5] and [5,5] ions, these ligands were apparently completely deprotonated, forming ruthenyl oxo groups. In addition to the [4,4] ion, below pH 2, the [4,5] ion became unstable with respect to disproportionation, so that the oxidation sequence reduced to

$$[3,3] \xrightarrow{-e^-} [3,4] \xrightarrow{3e^-} [5,5]$$

Some of the steps were electrochemically irreversible, which appeared to be a consequence of the kinetic complexity of their electrode reactions and/or instability associated with catalysis of water oxidation.[23] Consequently, it was not possible to confirm the assigned higher oxidation states by coulometry. Our earlier RR spectroscopic measurements gave provisional support for this general redox scheme.[10] Oxidative titration of the [3,3] ion with Co^{3+} ion in 0.1 M CF_3SO_3H gave three additional species, as detected from their strong ν_s(Ru—O—Ru) bands at 403, 393, and 370 cm^{-1}. The band at 403 cm^{-1} formed first, but was replaced by the 393-cm^{-1} band upon adding more Co^{3+}, which then diminished in intensity as the titration continued in favor of the 370-cm^{-1} band. In 1 M CF_3SO_3H, only two new species were detected, with ν_s(Ru—O—Ru) bands at ~400 and 360 cm^{-1}. By analogy with the electrochemical studies, the bands at 403, 393, and 370/360 cm^{-1} were assigned to the [3,4], [4,5], and [5,5] ions, respectively. The 370- to 360-cm^{-1} shift in ν_s(Ru—O—Ru) for the most highly oxidized species was attributed to protonation of the oxo bridge under strongly acidic conditions.

The absence of detectable EPR signals for the [3,3] ion is consistent with the bonding model presented in Figure 7a, where the HOMO is a fully occupied nondegenerate π^* orbital. Meyer and associates have found that the salts of several similar [3,3] μ-oxo ions, such as $[(Ru(bpy)_2NO_3)_2O](PF_6)_2$, were paramagnetic at room temperature and that below ~150 K their magnetic susceptibilities decreased with decreasing temperatures.[17] The magnetic data could be reproduced quantitatively by assuming that thermal equilibration occurred between the $^2\pi^*(p_y,d_{yz})$ singlet ground state and a low-lying $^1\pi^*(p_y,d_{yz})^1\pi^*(p_x,d_{xz})$ triplet excited state (Figure 7a). For the $(Ru(bpy)_2NO_3)_2O^{2+}$ ion, experimental parameters calculated from the Bleaney—Bowers equation[24] were $-2J = 173$ cm^{-1} for the separation of singlet and triplet energies, and $g_{av} = 2.48$. Extrapolation to very low temperatures using these parameters indicates that the complex is essentially diamagnetic below about 40 K. At that temperature, the calculated effective magnetic moment is $\mu_{eff}/Ru \simeq 0.2$ μ_B. Analogous behavior is expected for the $(Ru(bpy)_2H_2O)_2O^{4+}$ [3,3] ion, which would account for the lack of an EPR signal at these temperatures.

One-electron oxidation to the [3,4] ion caused appearance of a prominent anisotropic EPR signal (Figure 5), as expected for formation of an odd-spin paramagnetic ion. The spectral band shape was very similar to that previously observed for the [3,4] $[Ru(edta)]_2O^{3-}$ μ-oxo ion, although the peak position for that dimer was located at a lower magnetic field strength ($g_{max} = 2.40$).[25] The band position underwent pH-dependent shifts over regions that corresponded to deprotonation of coordinated *cis*-aqua ligands ($pK_{a_1} = 0.4$, $pK_{a_2} = 3.2$),[1] suggesting that the individual EPR bands with $g_{max} = 1.77$, 1.80, and 1.90 can be assigned to the discrete species $(Ru(bpy)_2OH_2)_2O^{5+}$, $[(bpy)_2(OH)Ru—O—Ru(OH_2)(bpy)_2]^{4+}$, and $(Ru(bpy)_2OH)_2O^{3+}$, respectively. This assignment cannot simultaneously account for the changes in relative intensities observed over the pH 0—3 region, however (Figure 5, inset). If the 370- to 360-cm^{-1} shift in ν_s noted for the putative [5,5] ion is correctly interpreted, then protonation of the bridging oxo ligand might also be expected for other oxidation states. Bridge protonation could, in principle, account for the complexity of the [3,4] signal in strongly acidic solutions, although identification of individual components could be difficult.

Several properties of the signal, including its high resistance to power saturation, the temperature dependence of its intensity, and possibly its extreme breadth, are indicative of rapidly relaxing electronic spin states. This behavior is consistent with expectations for an unpaired spin localized to the Ru—O—Ru center; because nuclear hyperfine splitting was not observed, it is difficult to assess from the available data the extent of spin delocalization over both metal centers. However, the position of the ν_s(Ru—O—Ru) PR band shifts from 371 cm^{-1} in the [3,3] ion to 402 cm^{-1} in the [3,4] ion, consistent with removal of an electron from a strongly antibonding orbital and, hence, with a delocalized orbital model.

The new band at $g = 1.87$ formed by oxidation of $(Ru(bpy)_2OH_2)_2O^{4+}$ with excess Ce^{4+} in 0.1 M CF_3SO_3H had a spectral band shape and relative intensity similar to the [3,4] ion (cf. Figures 5 and 6a). A reasonable assignment is the analogous [4,5] ion which, in the Raven and Meyer scheme,[6] is a $S = 1/2$ system with the odd electron spin residing in the doubly degenerate nonbonding d_{xy} orbital (Figure 7b). The sharp, nearly symmetric signal observed at $g = 1.95$ in 1 M CF_3SO_3H might then be assigned to a low-lying $^1\pi^n(d_{xz})^1\pi^n(d_{xy})$ triplet state of the [5,5] ion. If so, then the energy difference between the d_{xy} and d_{xz} orbitals must be very small in the [5,5] ion, since the signal persists to temperatures as low as 5 K. Alternatively, the signal might be attributable to the [4,4] ion which, according to the bonding scheme (Figure 7b),

(23) See, e.g., Dobson, J. C.; Meyer, T. J. *Inorg. Chem.* **1988**, *27*, 3283.

(24) Bleaney, B.; Bowers, K. *Proc. R. Soc. London, A* **1952**, *214*, 451.

(25) Zhou, J.; Xi, W.; Hurst, J. K. *Inorg. Chem.* **1990**, *29*, 160.

would exist in a $^2\pi^n(d_{xy})$ triplet ground state. However, this ion apparently does not accumulate since it has not been observed using either electrochemical or RR methods, techniques that should be capable of detecting this oxidation state at relatively low concentration levels. A more plausible assignment is that the $g = 1.95$ signal arises from a ligand radical ion. The signal band shape and position are strikingly similar to those of ligand radicals reported for reduced $Ru(bpy)_3^+$, $Ru(bpy)_3^0$, and $Ru(bpy)_3^-$ complexes and related species.[26-29] Specifically, the signal is nearly isotropic, its g value is close to the free-electron value, and the line width is relatively narrow (40 G) compared to that expected for metal-centered electrons. Although these properties alone do not establish the signal as arising from a ligand-centered $S = {}^1/_2$ system, they are certainly consistent with this assignment. Accordingly, the species giving rise to the signal could be the [5,5] π-cation radical. If the d_{xz}^n and d_{xy}^n orbital energies are inverted from the scheme given in Figure 7b, the [4,4] π-cation radical is also a possibility. However, this latter assignment implies the existence of the equilibrium [4,5] $\rightleftharpoons$ [4,4] π-cation, in which the odd electron is localized on metal-centered and bipyridine ligand-centered orbitals, respectively. Since the level of oxidation in these two species is the same, their relative concentrations should be independent of the overall redox poise of the system. This is not observed, however; the relative intensities of the $g = 1.87$-cm^{-1} RR band and $g = 1.95$ EPR signals vary with the amount of added Ce^{4+} ion (Figure 6b,c). Consequently, the [5,5] π-cation radical is the more likely assignment for the $g = 1.95$ signal.

The approximate correlation of intensities of the $g = 1.87$ EPR and 398-cm^{-1} ν_s(Ru—O—Ru) RR bands and $g = 1.95$ EPR and 817-cm^{-1} ν(Ru=O) RR bands, as well as the sequential progression of appearance of the bands upon oxidative titration, are evidence supporting assigning the 398-cm^{-1} ν_s(Ru—O—Ru) band to the [4,5] ion and the 817-cm^{-1} band to the [5,5] ion. Under the highest achievable oxidizing conditions, the excitation profiles for the 357- and 817-cm^{-1} RR bands were identical (Figure 4), supporting our earlier assignment of the 357-cm^{-1} band as ν_s(Ru—O—Ru) for the [5,5] ion. When the [3,4] ion is oxidized to the [4,5] ion, ν_s shifts from 402 to 398 cm^{-1}, despite removal of an antibonding $\pi^*(p_y,d_{yz})$ and a nonbonding d-electron from the Ru—O—Ru center. However, as previously mentioned, oxidation is accompanied by deprotonation of *cis*-aqua ligands,[1] promoting d_π—p_π overlap with the Ru d_{xz} and d_{xy} orbitals, as well as increasing σ-bonding interactions. These effects will destabilize the Ru—O—Ru $\pi^b(p_x,d_{xz})$ and σ-bonding orbitals in the bridge, leading to net weakening of the μ-oxo bond. The influence of *cis*-aqua ligand deprotonation within a single oxidation state is illustrated by the [3,4] ion, where ν_s is at 403 cm^{-1} for $(Ru(bpy)_2OH_2)_2O^{5+}$, 395 cm^{-1} for $[(bpy)_2(OH)Ru—O—Ru(OH_2)(bpy)_2]^{4+}$, and 392 cm^{-1} for $(Ru(bpy)_2OH)_2O^{3+}$ ion. Removing an additional d_π electron from the d_{xy} or d_{xz} orbital will increase competitive π-bonding to the terminal oxo atom, raising further the $\pi^b(p_x,d_{xz})$ orbital energy. Thus, when the [4,5] ion is oxidized to [5,5], ν_s lowers to 357 cm^{-1}.

Comparison to Earlier Studies. Collectively, the available data support the oxidation state assignments given for the individual ions and there is at least qualitative concurrence regarding their thermodynamic properties—specifically, that no direct evidence exists for accumulation of the [4,4] ion and, in strongly acidic media, the [4,5] ion is unstable with respect to its disproportionation to the [3,4] and [5,5] ions. Several important quantitative differences exist between our resonance Raman and EPR spectroscopic analyses[10] and the electrochemical studies of Meyer and associates,[1] however. One is that whereas they conclude that the [4,5] ion is unstable below pH 2, both RR[10] and EPR data (Figure 6a) clearly indicate nearly quantitative conversion of the [3,4] ion to [4,5] at pH 1. A second difference is that the observed EPR signals and changes in ν_s(Ru—O—Ru) and ν(Ru=O) RR bands upon oxidative titration with Ce^{4+} were not compatible with the presence of only four species (the [3,3], [3,4], [4,5], and [5,5] ions). Specifically, at intermediary levels of oxidation, appearance of significant absorption at ~360 cm^{-1} clearly preceded the appearance of the 817-cm^{-1} band (Figures 2 and 3) and, as discussed above, the $g = 1.95$ EPR signal is most probably attributable to a ligand radical-containing complex ion. Identifying causal relationships that might exist between the additional ~360-cm^{-1} RR band and the $g = 1.95$ EPR signal will require additional quantitative study. Finally, the protic equilibria in the strongly acidic domain appear to be more complex than originally envisioned. This conclusion is supported by the observations that the ν_s(Ru—O—Ru) for the [5,5] ion shifts from 370 to 360 cm^{-1} upon increasing the acidity from pH 1 to pH 0, that no ν(Ru=O) was observed for the [4,5] ion (suggesting that the *cis*-oxo ligands are protonated, contrary to earlier conclusions), and that the EPR spectral shifts of the [3,4] ion cannot be explained terms of protic equilibria involving just the *cis*-aqua ligands. These differences are perhaps not surprising when one realizes that the systems being studied are not in thermodynamic equilibrium. The electrochemical measurements are difficult to interpret because several of the oxidation steps are irreversible,[5,31] and in general, all measurements were made upon dynamic systems undergoing catalytic turnover. Consequently, steady-state concentration levels of intermediates were determined, which are nonequilibrium values whose displacement from equilibrium will vary under different reaction conditions.

Mechanistic Implications. In studies reported elsewhere, we have examined the initial rates of $[(bpy)_2Ru(OH_2)]_2O$-catalyzed water oxidation by Co^{3+} ion.[32] These studies indicate that the reaction is unimolecular with respect to the catalyst and that the O_2-evolving oxidation state must be higher than the [4,5] ion. Consequently, the higher oxidation states detected by RR and EPR methods may be important components of the catalytic cycle. In this context, the appearance of a ligand radical cation-containing species is intriguing because it suggests functional analogies to biological water oxidation. In the oxygen-evolving complex (OEC) of photosystem II, most of the available physical data[33-36] has been interpreted to indicate that the penultimate oxidation step in the catalytic cycle ($S_2 \rightarrow S_3$ in the Kok scheme[37]) involves oxidation at a site other that

(26) Motten, A. G.; Hanck, K.; DeArmond, M. K. *Chem. Phys. Lett.* **1981**, *79*, 541.
(27) Morris, D. E.; Hanck, K. W.; DeArmond, M. K. *J. Am. Chem. Soc.* **1983**, *105*, 3032.
(28) Morris, D. E.; Hanck, K. W.; DeArmond, M. K. *Inorg. Chem.* **1985**, *24*, 977.
(29) Poppe, J.; Moscherosch, M.; Kaim, W. *Inorg. Chem.* **1993**, *32*, 2640.
(30) Kaim, W. *Coord. Chem. Rev.* **1987**, *76*, 187.
(31) Diamantis, A. A.; Murphy, W. R.; Meyer, T. J. *Inorg. Chem.* **1984**, *23*, 3230.
(32) Lei, Y.; Hurst, J. K. *Inorg. Chim. Acta*, in press.
(33) Guiles, R. D.; Zimmerman, J.-L.; McDermott, A. E.; Yachandra, V. K.; Cole, J. L.; Dexheimer, S. L.; Britt, R. D.; Weighardt, K.; Bossek, U.; Sauer, K.; Klein, M. P. *Biochemistry* **1990**, *29*, 471.
(34) Baumgarten, M.; Philo, J. S.; Dismukes, G. C. *Biochemistry* **1990**, *29*, 10814.
(35) Srinivasan, A. N.; Sharp, R. R. *Biochim. Biophys. Acta* **1986**, *851*, 369.
(36) See, however: Dekker, J. P. In *Manganese Redox Enzymes*; Pecoraro, V. L., Ed.; VCH Publishers: New York, 1992; p 85.

the Mn cluster (whereas all other steps involve Mn oxidation). An EPR signal detected in Ca^{2+}-depleted membranes oxidized to the level of the S_3 state has been assigned to a histidyl radical in proximity to the Mn cluster within the OEC binding pocket.[38,39] Thus, the catalytic mechanisms of water oxidation by ruthenium μ-oxo ions may be useful models for understanding the corresponding biological reactions.

Acknowledgment. This research was supported by the Office of Basic Energy Sciences, U.S. Department of Energy, under Grant DE-FG-06-87ER-13664. The authors are also grateful to Professor Thomas M. Loehr for making available to us his Raman facility.

(37) Kok, B.; Forbush, B.; McGloin, M. *Photochem. Photobiol.* **1970**, *11*, 457.
(38) Boussac, A.; Zimmerman, J.-L.; Rutherford, A. W.; Lavergne, J. *Nature* **1990**, *347*, 303.
(39) Ono, T.; Inoue, Y. *FEBS Lett.* **1991**, *278*, 183.